



New switch on fluorescent probe with AIE characteristics for selective and reversible detection of mercury ion in aqueous solution

Yanglei Yuan^a, Xin Chen^a, Qing Chen^b, Guoyu Jiang^{c,d}, Hongmei Wang^{a,*}, Jianguo Wang^{c,d,**}

^a Department of Applied Chemistry, China Agricultural University, Beijing, 100193, PR China

^b College of Resource and Environmental Science, China Agricultural University, 100193, Beijing, China

^c College of Chemistry and Chemical Engineering, Inner Mongolia University, Hohhot, 010021, PR China

^d Key Laboratory of Organo-Pharmaceutical Chemistry, Gannan Normal University, Ganzhou, 341000, PR China

ARTICLE INFO

Keywords:

Mercury
Fluorescent probe
Aggregation-induced emission
Switch on
Reversible detection

ABSTRACT

A new tetraphenylethylene derivative based fluorescent probe (probe 2) was synthesized in a simple two-step process for selectively switch on and reversible detection of Hg^{2+} in aqueous solution based on aggregation-induced emission phenomenon. Probe 2 exhibited weak emission in aqueous solution due to the fast non-radiative decay of the excited singlet state facilitated by the free rotation of four phenyl rotors. While after coordination with Hg^{2+} , the Hg^{2+} -promoted aggregation formation will occur and restrict the intramolecular rotation, which blocks the non-radiative pathways and opens up the emission channel, resulting in the switch on response of probe 2 toward Hg^{2+} . Probe 2 exhibited high sensitivity and good selectivity toward Hg^{2+} with a detection limit of 45.4 nM. Moreover, the detection can be reversible by subsequent addition of S^{2-} into the detection system, which may be applied in the removal of toxic Hg^{2+} from water. Elsevier B.V. All rights reserved.

1. Introduction

As a heavy and transition metal ion, mercury (Hg^{2+}) is considered to be highly toxic and dangerous to human health and the environment [1]. Environmental Hg^{2+} can be easily converted by aerobic organisms to more toxic methylmercury, which can readily enter biological membranes due to their lipid solubility, leading to severe neurotoxicity to many eukaryotes including fish, animals and finally humans through food-chain accumulation [2]. Nowadays, Hg^{2+} has severely contaminated water, air, land and the food chain due to man-made activities [3]. And long exposure to high levels of Hg^{2+} may result in lasting and highly harmful effects in biological systems, causing various diseases including cognitive and motion disorders, language, hearing, vision and hair loss, prenatal neuron and brain damage, Minamata disease and even death [4,5]. Due to the high threat of Hg^{2+} to human beings, the maximum allowed amount of Hg^{2+} in drinking water (2 ppb, ca. 10 nM) was set by the U.S. Environmental Protection Agency (EPA) [6], which also manifested the great significance of developing reliable methods for the highly sensitive and selective detection of Hg^{2+} in aqueous solutions.

Traditional detection methods for Hg^{2+} , such as gas

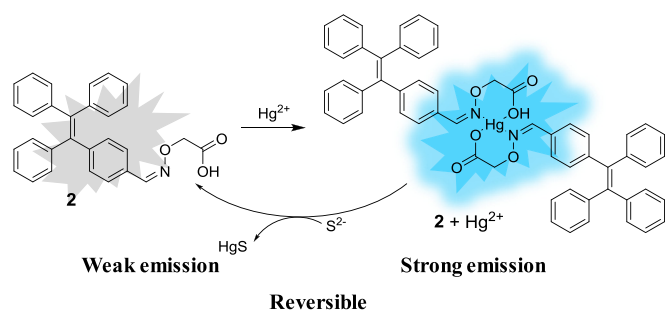
chromatography (GC), high performance liquid chromatography (HPLC), inductively coupled plasma mass spectrometry (ICP MS), X-ray fluorescence spectrophotometry, atomic absorption spectroscopy (AAS), and neutron activation analysis [7–11], may greatly suffer from costly and complicated equipments, long data acquisition time and/or the involvement of skilled personnel. Fluorescent probes, featured with the unique advantages of high specificity and sensitivity, simple operation, non-invasiveness and applicability to real-time and online bioimaging, have aroused great interest in the rapid and convenient assay of various analytes, especially biologically relevant species [12–21]. A large number of fluorescent probes have already been reported in recent years to realize the easy and quick sensing of Hg^{2+} [22–27]. However, the OFF response could not be differentiated with the false signal induced by quenching of Hg^{2+} . Moreover, most fluorescent probes for Hg^{2+} were fabricated based on traditional aggregation-caused quenching (ACQ) fluorophores, which may also bring about interference from the quenching of emission in high concentration solutions or after they accumulated in cells [28,29].

To prevail the ACQ effect, the concept of aggregation-induced emission (AIE) was put forward by Tang et al., in 2001 [28,29]. The AIE Luminogens (AIEgens) exhibit opposite emission behaviours compared

* Corresponding author.

** Corresponding author. College of Chemistry and Chemical Engineering, Inner Mongolia University, Hohhot, 010021, PR China.

E-mail address: whmd@cau.edu.cn (H. Wang).



Scheme 1. Schematic representation of switch on and reversible detection of Hg^{2+} by probe **2** in aqueous solutions.

to traditional ACQ fluorophores, that is, they are weakly or non-emissive in solution but give bright emission in the aggregation and solid state. The AIE mechanism has mainly been attributed to the restriction of intramolecular motion (RIM), which blocks the non-radiative pathways and opens up the emission channel in the aggregation state [30–34]. By now, numerous fascinating AIE probes for various biological-relevant species such as, metal ions, proteins, DNA, enzymes, have been fabricated through well tuning of the aggregation/disaggregation conditions of AIEgens [30–34]. In fact, a number of fluorescent probes for Hg^{2+} have been developed based on AIEgens [35–45]. However, most of the AIE sensors still exist some drawbacks such as low sensitivity, switch off response and poor practicability which required a much high content of organic solvents in aqueous solutions to afford proper handling of the detection process [46–53]. Fluorescent probes with the features of rapid, sensitive, highly selective and reversible detection of Hg^{2+} in aqueous solution through a switch on mode is still in high demand.

Herein, we designed a new AIE fluorescent probe (probe **2** in Scheme 1) for switch on and reversible detection of Hg^{2+} in aqueous solution. As shown in Scheme 1, we chose 2-(aminoxy)acetic acid as a chelator for Hg^{2+} . The reaction between 2-(aminoxy)acetic acid and 4-(1,2,2-triphenylvinyl)benzaldehyde (shown in Scheme 2) can easily afford a Schiff base compound **2** with high yield (92%). Fortunately, probe **2** was rendered some water solubility due to the presence of carboxylic acid group, which is favorable for its application in biological and environmental samples. Moreover, the emission of probe **2** in aqueous solution was very weak due to the rotation of phenyl rings. While after coordinated with Hg^{2+} , the Hg^{2+} -promoted aggregation

formation will occur and restrict the intramolecular rotation, which blocks the non-radiative pathways and opens up the emission channel, resulting in the switch on response of probe **2** toward Hg^{2+} . Probe **2** exhibited high sensitivity and good selectivity toward Hg^{2+} with a detection limit of 45.4 nM. What's more, the detection can be reversible by subsequent addition of S^{2-} into the detection system, which may be applied in the removal of toxic Hg^{2+} from water.

2. Experimental

2.1. General information

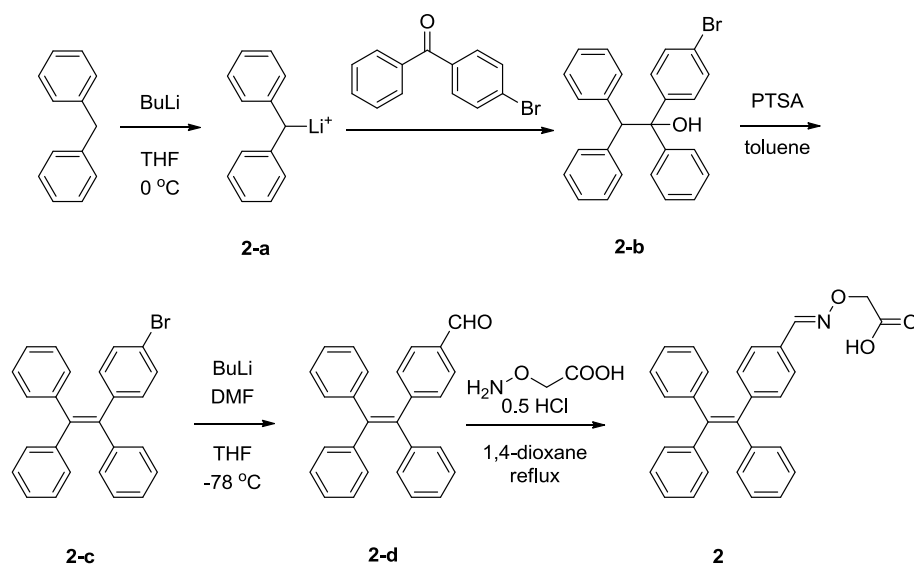
All solvents were purified and dried following standard procedures unless special statements. Other chemical reagents were commercial available and used as received.

^1H NMR spectra were obtained on a Bruker DMX-300MHz spectrophotometer. High resolution mass spectra were obtained on Bruker APEX IV (7.0 T) FT-MS. UV-Vis absorption spectra and fluorescence emission spectra were recorded on a Shimadzu UV-1601PC spectrophotometer and a Hitachi F-4500 fluorescence spectrophotometer, respectively. Dynamic light scattering (DLS) experiments were carried out with Malvern Instrument (Nano Series). Confocal fluorescence imaging experiments were performed with an Olympus FV-1000 laser scanning microscopy system, based on an IX81 (Olympus, Japan) inverted microscope. The microscope was equipped with 375 nm (CW) laser lines and UPLSAPO 60x/N.A 1.42 objective. Images were collected and processed with Olympus FV10-ASW Ver.2.1b software.

2.2. Synthesis

2.2.1. Compound 2-b

To a THF solution (100 mL) of diphenylmethane (18.0 g, 107 mmol) at 0°C was added a solution of *n*-BuLi in hexane (2.5 M). The mixture was stirred for 30 min to result in an orange solution of **2-a**. To the solution of **2-a**, (4-bromophenyl) (phenyl)methanone (26.1 g, 100 mmol) was added at 0°C . After that, the mixture was continuously stirred at room temperature for another 6 h. Saturated NH_4Cl was added to quench the reaction. The reaction mixture was filtered under reduced pressure and the resultant was dried to obtain compound **2-b**. Compound **2-b** (36.0 g, 84 mmol) was dissolved in 10 mL of toluene and *p*-toluenesulfonic acid was added as a catalyst. The reaction mixture was refluxed overnight and purified by silica chromatography using ethyl acetate and petroleum ether (1/100, v/v) as the eluent. Yield:



Scheme 2. Synthetic route of probe **2**.

96%.

To a solution of compound **2-c** in 15 mL of THF at $-78\text{ }^{\circ}\text{C}$, *n*-BuLi (3 mL, 1.6 M, 4.86 mmol) in hexane (3 mL) was added dropwise. The mixture was stirred at $-78\text{ }^{\circ}\text{C}$ for 2 h before quickly adding anhydrous DMF (1.1 mL, 14.56 mmol). The mixture was stirred at temperature for another 6 h. The mixture was washed with brine and extracted with dichloromethane twice. The organic layer was combined and dried over anhydrous Na_2SO_4 , filtered and evaporated. The residue was subjected to column chromatography with ethyl acetate/petroleum ether (95/5, v/v) as eluent to obtain compound **2-d** as a solid. Yield: 45%. $^1\text{H NMR}$ (300 MHz, CDCl_3) δ 9.92 (s, 1H), 7.64 (d, $J = 8.3\text{ Hz}$, 2H), 7.23 (d, $J = 8.2\text{ Hz}$, 2H), 7.17–7.10 (m, 9H), 7.09–7.02 (m, 6H). $^{13}\text{C NMR}$ (75 MHz, CDCl_3) δ 191.51, 150.22, 142.73, 142.68, 142.58, 139.46, 133.99, 131.62, 130.97, 130.95, 130.91, 128.83, 127.62, 127.61, 127.43, 126.73, 126.57, 126.54.

2.2.2. Compound 2

Compound **2-d** (0.30 g, 0.80 mmol) and 2-(aminoxy)acetic acid (0.115 g, 1.26 mmol) was added to 30 mL redistilled 1,4-dioxane in order. The reaction mixture was refluxed for 2.5 h. After cooling to room temperature, the mixture was washed with brine and extracted with ethyl acetate twice. The organic layer was combined and dried over anhydrous Na_2SO_4 , filtered and evaporated. The residue was subjected to column chromatography with ethyl acetate/petroleum ether (1/20–1/2, v/v) as eluent. Compound **2** was obtained as a light yellow solid. Yield: 92%. $^1\text{H NMR}$ (300 MHz, CDCl_3) δ 8.11 (s, 1H), 7.32 (d, $J = 8.3\text{ Hz}$, 2H), 7.15–7.08 (m, 9H), 7.07–6.98 (m, 8H), 4.73 (s, 2H); $^{13}\text{C NMR}$ (75 MHz, DMSO) δ 174.87, 150.46, 146.02, 143.25, 143.18, 143.09, 141.76, 139.99, 131.55, 131.14, 131.10, 129.05, 127.66, 127.59, 127.50, 126.60, 126.45, 77.05. HRMS m/z calculated for $\text{C}_{29}\text{H}_{24}\text{NO}_3^+$: $[\text{M} + \text{H}]^+$ 434.1751, found 434.1754.

2.3. Determination of the detection limit of probe 2 toward addition of Hg^{2+}

Based on the linear fitting in Fig. 1B, the detection limit (C) is estimated as follows:

$$C = 3\sigma/B$$

Where σ is the standard deviation obtained from three individual fluorescence measurements ($I_{478\text{ nm}}$) of probe **2** ($25\text{ }\mu\text{M}$) without Hg^{2+} and B is the slope obtained after linear fitting the titration curves within certain ranges.

3. Results and discussion

3.1. Synthesis and characterization

Probe **2** can be easily prepared and purified according to reported method (Scheme 2) [54]. The chemical structures of probe **2** and intermediate compounds were confirmed by standard spectroscopy methods with satisfactory results. Details of synthesis and characterization can be found in Figs. S4–S8 in the supplementary materials.

3.2. The AIE behavior of probe 2

The AIE properties of probe **2** was confirmed in ethanol/water mixtures with different water volume fractions (f_w). Results from Fig. S1 in the supplementary materials showed that the emission of probe **2** was very weak in ethanol and increased slowly until f_w reached 70%. Then the emission intensified swiftly, especially when f_w was beyond 80%. As water is a poor solvent for probe **2**, the addition of water will induce the formation of probe **2** aggregates, and thus turned on the emission. As a result, probe **2** features the unique AIE characteristics. Moreover, the behavior of probe **2** in high concentration solutions also confirmed its AIE feature. As depicted in Fig. S2, the emission intensity of probe **2** in pure water gradually enhanced as its concentration increased. Again, with water as a poor solvent for probe **2**, the concentration increase will induce the formation of more and more aggregates, which blocked the non-radiative decay pathway, and turned on the emission, similar to those of reported TPE derivatives [30–34].

3.3. The spectra response of probe 2 toward Hg^{2+}

To validate our initial design concept for switch on detection of Hg^{2+} , the spectra response of probe **2** toward Hg^{2+} were first recorded in ethanol/water mixture (3/7, v/v). As depicted in Fig. 1A, probe **2** was weakly emissive in the absence of Hg^{2+} . While after the addition of Hg^{2+} , the blue emission was greatly switched on with a peak centered at 478 nm, due to the Hg^{2+} -promoted aggregation formation. The emission intensity gradually enhanced with increasing aliquots of Hg^{2+} . Moreover, a good linearity was found between the emission intensity of probe **2** and the concentration of Hg^{2+} with a range of 15–45 μM (Fig. 1B). The limit of detection was thus calculated to be 45.4 nM, based on the $3\sigma/B$ rule (where σ is the standard deviation of blank measurements and B is the slope of the linear equation) [54]. The detection mechanism was proposed as shown in Scheme 1. In the absence of Hg^{2+} , probe **2** can be well dissolved in ethanol/water mixture (3/7, v/v), without forming aggregates. While after addition of Hg^{2+} , the $-\text{CH}=\text{N}$ and $-\text{OH}$ group can coordinate with Hg^{2+} , resulting in $2 + \text{Hg}^{2+}$ complex with poor water solubility. And as a result,

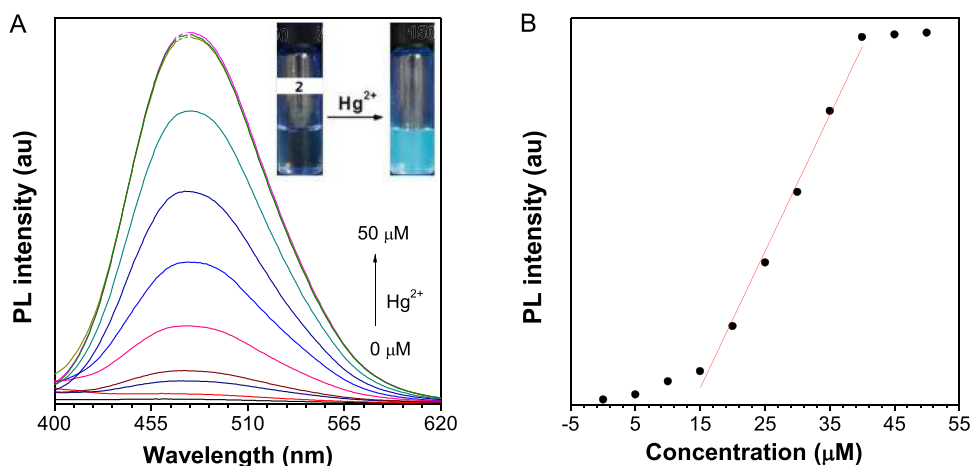


Fig. 1. (A) Fluorescent emission spectra of probe **2** ($25.0\text{ }\mu\text{M}$ in ethanol/water mixture, 3/7, v/v) before and after addition of different concentrations of Hg^{2+} ($0.0\text{--}52.0\text{ }\mu\text{M}$). Inset: fluorescent photographs of probe **2** before and after addition of $50.0\text{ }\mu\text{M}$ Hg^{2+} taken under 365 nm UV irradiation. (B) The plot and linear fitting of fluorescence intensity of probe **2** ($25.0\text{ }\mu\text{M}$) at 478 nm as a function of the concentration of Hg^{2+} . Excitation wavelength ($\lambda_{\text{ex}} = 330\text{ nm}$).

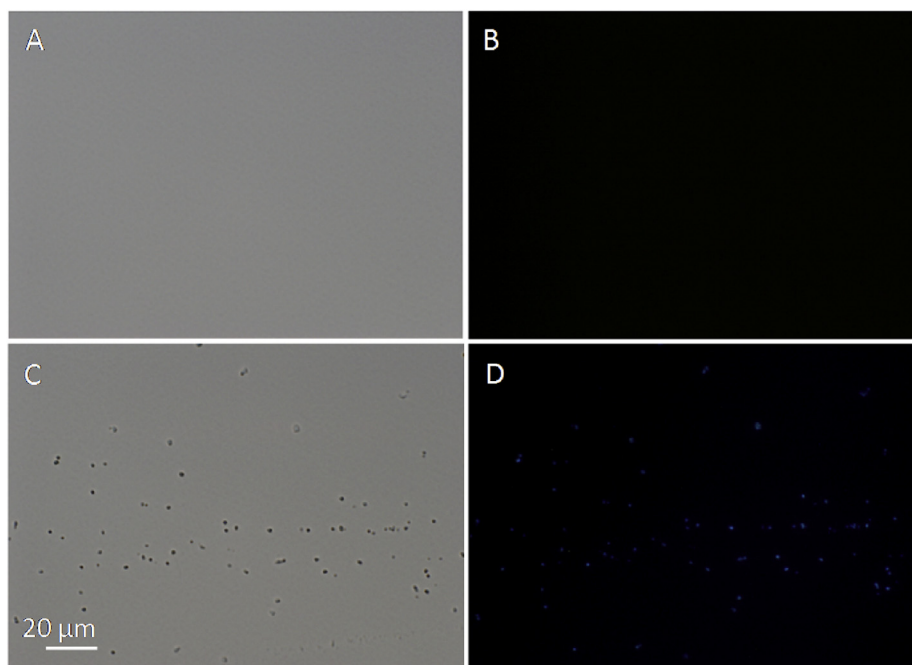


Fig. 2. Fluorescence microscope images of probe **2** (25.0 μM) in $\text{H}_2\text{O}/\text{EtOH}$ mixture in the absence (A and B) and presence (C and D) of Hg^{2+} (50.0 μM). Scale bar represents 20 μm . Excitation was set at 405 nm.

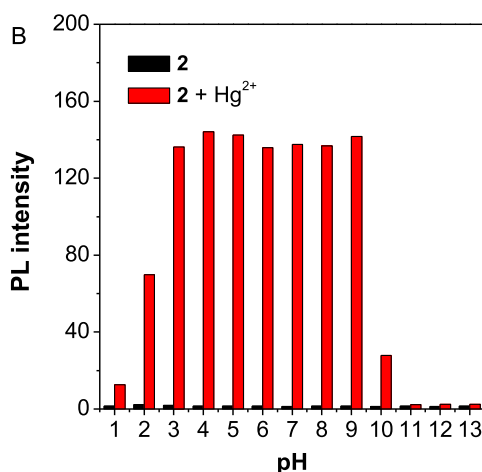
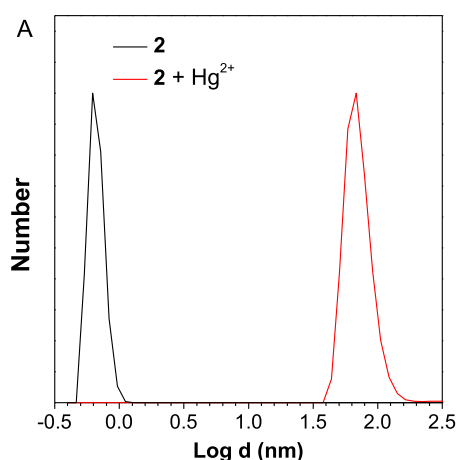


Fig. 3. (A) DLS data of probe **2** before and after addition of 50.0 μM Hg^{2+} . (B) Fluorescence intensity at 478 nm of probe **2** (black bars) and probe **2** + Hg^{2+} (red bars) at different pH value in buffered solution. $\lambda_{\text{ex}} = 330$ nm. (For interpretation of the references to colour in this figure legend, the reader is referred to the Web version of this article.)

aggregation will occur and turn on the emission. To confirm the proposed detection mechanism, both fluorescence imaging and dynamic light scattering (DLS) experiments were carried out. As illustrated in Fig. 2, the solution of probe **2** exhibited negligible emission before the addition of Hg^{2+} . However, in the presence of Hg^{2+} , light blue dots can be clearly observed in the fluorescence imaging. DLS data also indicated the formation of 20–200 nm aggregates for the mixed solution of probe **2** and Hg^{2+} (Fig. 3A). To ascertain the actual binding stoichiometry of the probe **2**- Hg^{2+} conjugate, a Job's plot analysis was conducted. As shown in Fig. S3, the emission intensity changes at 478 nm versus the mole fraction of Hg^{2+} was measured. The maximum emission intensity change was observed at a mole fraction of about 0.33, which supported a 2:1 complex formed between probe **2** and Hg^{2+} . According to these results, the detection mechanism was proposed as shown in Scheme 1.

3.4. pH effect

The influence of pH on the properties of probe **2** and its response to

Hg^{2+} was also evaluated, as the pH values in different samples to be tested may vary drastically. As shown in Fig. 3B, the fluorescence intensity of probe **2** is stable within a wide pH range from 1.0 to 13.0. However, the response of probe **2** toward Hg^{2+} showed the highest sensitivity in pH 3.0–9.0. More acidic or alkaline media would result in poor fluorescence response, probably due to the poor coordination ability of probe **2** with Hg^{2+} in strong acidic conditions, or the formation of $\text{Hg}(\text{OH})_2$ at basic pHs [41].

3.5. Selectivity

To check the specificity of probe **2** toward Hg^{2+} , we then evaluated the responses of probe **2** toward common metal ions in parallel under the same conditions. As exhibited in Fig. 4, the addition of Hg^{2+} induced a prominent enhancement of the PL intensity, while other metal ions including Ag^+ , Au^{3+} , Ba^{2+} , Ca^{2+} , Cd^{2+} , Co^{2+} , Cr^{3+} , Cu^{2+} , Fe^{2+} , Fe^{3+} , K^+ , Li^+ , Mg^{2+} , Mn^{2+} , Na^+ , Ni^{2+} , Pd^{2+} , Pt^{2+} , Rh^{3+} , Zn^{2+} , Zr^{4+} caused no changes, except for Pb^{2+} , which lead to a small emission enhancement. The high sensitivity of probe **2** toward Hg^{2+} might be

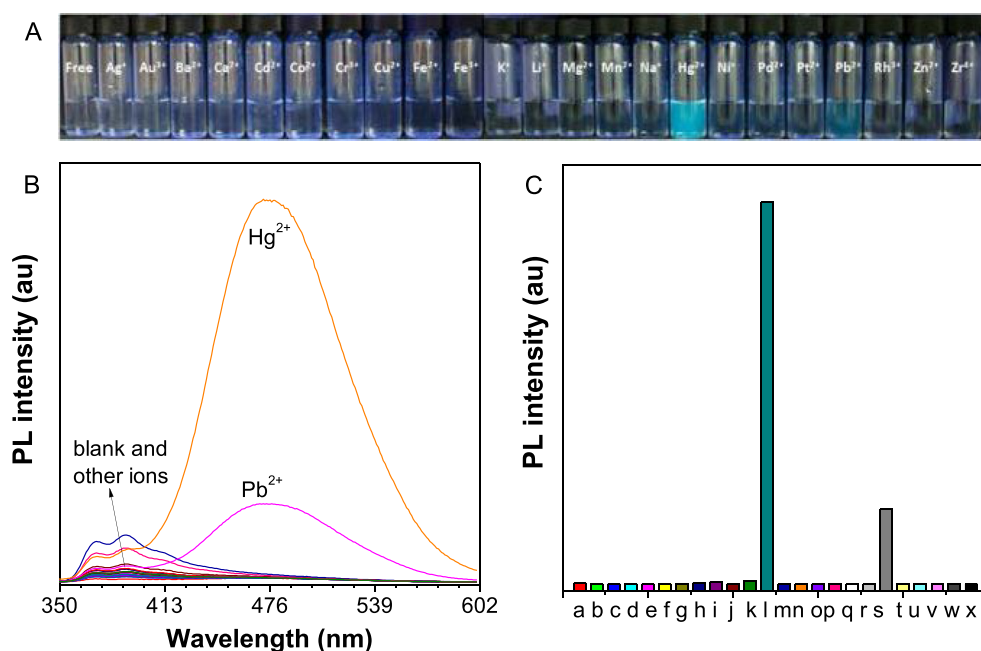


Fig. 4. (A) Fluorescent photographs of probe 2 (25.0 μM , $\text{H}_2\text{O}/\text{EtOH} = 7/3$) before and after addition of various common metal ions taken under 365 nm UV irradiation. (B) The fluorescence spectra of probe 2 in the presence of various common metal ions. (C) The fluorescence intensity changes of probe 2 at 478 nm in the presence of various common metal ions. a: blank; b: Ag^+ ; c: Au^{3+} ; d: Ba^{2+} ; e: Ca^{2+} ; f: Cd^{2+} ; g: Co^{2+} ; h: Cr^{3+} ; i: Cu^{2+} ; j: Fe^{2+} ; k: Fe^{3+} ; l: Hg^{2+} ; m: K^+ ; n: Li^+ ; o: Mg^{2+} ; p: Mn^{2+} ; q: Na^+ ; r: Ni^{2+} ; s: Pb^{2+} ; t: Pd^{2+} ; u: Pt^{2+} ; v: Rh^{3+} ; w: Zn^{2+} ; x: Zr^{4+} . The concentration of Hg^{2+} and Pb^{2+} is 50.0 μM , while concentrations of other metal ions are 100 μM , $\lambda_{\text{ex}} = 330 \text{ nm}$.

Table 1
Detection of Hg^{2+} in tap water.

Method	Added (μM)	Detected (μM)	Recovery (%)	RSD (%)
ICP-MS	0	Not detected	/	/
	30.00	30.17	100.6	2.6
Probe 2	0	Not detected	/	/
	30.00	30.93	103.1	1.1

due to the fact that mercury ion has a higher binding affinity and faster chelating kinetics with N and O functional groups in probe 2 than Pb^{2+} and other metal ions [27]. These results demonstrated a good selectivity of probe 2 toward Hg^{2+} .

3.6. Analysis of Hg^{2+} in real sample

The fluorescent probe 2 has been validated for practical application in the determination of Hg^{2+} ion content in tap water. Control experiments show that no Hg^{2+} was detected in tap water. When Hg^{2+} was added, fluorescence spectra were recorded and the contents of Hg^{2+} ions were recovered using the linear equation obtained from Fig. S4. Table 1 presents the results and good recoveries were obtained. In order to demonstrate the accuracy of this method, the results were compared to those obtained by ICP-MS. As shown in Table 1, results obtained by probe 2 agrees well with those obtained by ICP-MS, indicating that the proposed method can be used to analyze Hg^{2+} accurately.

3.7. Reversibility

The reversibility of the detection process was further investigated by the addition of S^{2-} to the probe 2 + Hg^{2+} complex. Owing to the much stronger binding affinity of Hg^{2+} to S^{2-} , S^{2-} can deplete Hg^{2+} from probe 2 + Hg^{2+} complex, releasing free probe 2, which recovers its weak emission (Fig. S5 in supplementary information). The reversibility of probe 2 toward Hg^{2+} detection may expand the application of probe 2 to the removal of toxic Hg^{2+} from environmental samples.

4. Conclusion

We have successfully established a switch on and reversible fluorescent probe for the sensitive detection of Hg^{2+} in aqueous solution based on the unique AIE behaviour of a tetraphenylethylene derivative (probe 2). Probe 2 exhibited high sensitivity and good selectivity toward Hg^{2+} with a detection limit of 45.4 nM. The reversibility of probe 2 toward Hg^{2+} detection may also extend the application of probe 2 to the removal of toxic Hg^{2+} from tap water or environmental samples.

Acknowledgments

This work was supported by China Agriculture Research System (CARS-23-B16), The National Key R&D Program of China (2016YFD0801006), National Natural Science Foundation of China (21663005 and 21871060), and the Natural Science Foundation of Jiangxi Province (2018ACB21009, 20181BAB213007).

Appendix A. Supplementary data

Supplementary data to this article can be found online at <https://doi.org/10.1016/j.ab.2019.113403>.

References

- [1] E.M. Nolan, S.J. Lippard, Tools and tactics for the optical detection of mercuric ion, *Chem. Rev.* 108 (9) (2008) 3443–3480.
- [2] M. McNutt, Taming a mercurial element, *Science* 341 (6153) (2013) 1442–1443.
- [3] J. Qiu, Tough talk over mercury treaty, *Nature* 493 (2013) 144–145.
- [4] F. Wang, S.W. Nam, Z. Guo, S. Park, J. Yoon, A new rhodamine derivative bearing benzothiazole and thiocarbonyl moieties as a highly selective fluorescent and colorimetric chemodosimeter for Hg^{2+} , *Sens. Actuators B Chem.* 161 (1) (2012) 948–953.
- [5] B. Weiss, Why methylmercury remains a conundrum 50 years after minamata, *Toxicol. Sci.* 97 (2) (2007) 223–225.
- [6] Mercury Update: Impact on Fish Advisories, EPA, Office of Water, Washington, DC, 2001, pp. 1–10 EPA Fact Sheet EPA-823-F-01-011.
- [7] M. Wang, W. Feng, J. Shi, F. Zhang, B. Wang, M. Zhu, B. Li, Y. Zhu, Z. Chai, Development of a mild mercaptoethanol extraction method for determination of mercury species in biological samples by HPLC-ICP-MS, *Talanta* 71 (5) (2007) 2034–2039.
- [8] N. Demuth, K.G. Heumann, Validation of methylmercury determinations in aquatic systems by alkyl derivatization methods for GC analysis using ICP-IDMS, *Anal. Chem.* 73 (16) (2001) 4020–4027.
- [9] I. Narin, M. Soylyak, L. Elci, M. Doğan, Determination of trace metal ions by AAS in

- natural water samples after preconcentration of pyrocatechol violet complexes on an activated carbon column, *Talanta* 52 (6) (2000) 1041–1046.
- [10] H. Zheng, B. Jia, Z. Zhu, Z. Tang, S. Hu, Determination of trace amounts of Pb, Cd, Ni and Co by wavelength-dispersive X-ray fluorescence spectrometry after preconcentration with dithizone functionalized graphene, *Anal. Methods* 6 (21) (2014) 8569–8576.
- [11] E. Witkowaska, K. Szczepaniak, M. Biziuk, Some applications of neutron activation analysis, *J. Radioanal. Nucl. Chem.* 265 (1) (2005) 141–150.
- [12] B. Dong, X. Song, X. Kong, C. Wang, N. Zhang, W. Lin, Two-photon red-emissive fluorescent probe for imaging nitroxyl (HNO) in living cells and tissues, *J. Mater. Chem. B* 5 (26) (2017) 5218–5224.
- [13] K. Hanaoka, K. Kikuchi, S. Kobayashi, T. Nagano, Time-resolved long-lived luminescence imaging method employing luminescent lanthanide probes with a new microscopy system, *J. Am. Chem. Soc.* 129 (44) (2007) 13502–13509.
- [14] S. Gan, J. Zhou, T.A. Smith, H. Su, W. Luo, Y. Hong, Z. Zhao, B.Z. Tang, New AIEgens with delayed fluorescence for fluorescence imaging and fluorescence lifetime imaging of living cells, *Mater. Chem. Front.* 1 (12) (2017) 2554–2558.
- [15] D. Wu, A.C. Sedgwick, T. Gunnlaugsson, E.U. Akkaya, J. Yoon, T.D. James, Fluorescent chemosensors: the past, present and future, *Chem. Soc. Rev.* 46 (23) (2017) 7105–7123.
- [16] Y. Fang, W. Shi, Y. Hu, X. Li, H. Ma, A dual-function fluorescent probe for monitoring the degrees of hypoxia in living cells via the imaging of nitroreductase and adenosine triphosphate, *Chem. Commun.* 54 (43) (2018) 5454–5457.
- [17] X. Hou, J. Peng, F. Zeng, C. Yu, S. Wu, An anthracenecarboximide fluorescent probe for in vitro and in vivo ratiometric imaging of endogenous alpha-L-fucosidase for hepatocellular carcinoma diagnosis, *Mater. Chem. Front.* 1 (4) (2017) 660–667.
- [18] C.-J. Zhang, X. Cai, S. Xu, R. Zhan, W. Jien, B. Liu, A light-up endoplasmic reticulum probe based on a rational design of red-emissive fluorogens with aggregation-induced emission, *Chem. Commun.* 53 (78) (2017) 10792–10795.
- [19] H. Xu, Q. Li, L. Wang, Y. He, J. Shi, B. Tang, C. Fan, Nanoscale optical probes for cellular imaging, *Chem. Soc. Rev.* 43 (8) (2014) 2650–2661.
- [20] P. Verwilst, H.S. Kim, S. Kim, C. Kang, J.S. Kim, Shedding light on tau protein aggregation: the progress in developing highly selective fluorophores, *Chem. Soc. Rev.* 47 (7) (2018) 2249–2265.
- [21] S. Uno, M. Kamiya, A. Morozumi, Y. Urano, A green-light-emitting, spontaneously blinking fluorophore based on intramolecular spirocyclization for dual-colour super-resolution imaging, *Chem. Commun.* 54 (1) (2018) 102–105.
- [22] G. Chen, Z. Guo, G. Zeng, L. Tang, Switching specific biomolecular interactions on surfaces under complex biological conditions, *Analyst* 140 (21) (2015) 5400–5443.
- [23] N. Kumar, V. Bhalla, M. Kumar, Resonance energy transfer-based fluorescent probes for Hg^{2+} , Cu^{2+} and Fe^{2+}/Fe^{3+} ions, *Analyst* 139 (3) (2014) 543–558.
- [24] J. Du, M. Hu, J. Fan, X. Peng, Fluorescent chemodosimeters using “mild” chemical events for the detection of small anions and cations in biological and environmental media, *Chem. Soc. Rev.* 41 (12) (2012) 4511–4535.
- [25] H.N. Kim, W.X. Ren, J.S. Kim, J. Yoon, Fluorescent and colorimetric sensors for detection of lead, cadmium, and mercury ions, *Chem. Soc. Rev.* 41 (8) (2012) 3210–3244.
- [26] A. Badiie, B.V. Razavi, H. Goldoos, G.M. Ziarani, F. Faridbod, M.R. Ganjali, A novel fluorescent chemosensor assembled with 2,6-bis(2-benzimidazolyl)pyridine-functionalized nanoporous silica-type SBA-15 for recognition of Hg^{2+} ion in aqueous media, *Int. J. Environ. Res.* 12 (1) (2018) 109–115.
- [27] G. Shiravand, A. Badiie, G.M. Ziarani, Carboxyl-rich $g-C_3N_4$ nanoparticles: synthesis, characterization and their application for selective fluorescence sensing of Hg^{2+} and Fe^{3+} in aqueous media, *Sens. Actuators B Chem.* 242 (2017) 244–254.
- [28] D. Ding, K. Li, B. Liu, B.Z. Tang, Bioprobes based on AIE fluorogens, *Acc. Chem. Res.* 46 (11) (2013) 2441–2453.
- [29] Y. Zhao, R.T.K. Kwok, J.W.Y. Lam, B.Z. Tang, A highly fluorescent AIE-active theranostic agent with anti-tumor activity to specific cancer cells, *Nanoscale* 8 (25) (2016) 12520–12523.
- [30] Z. He, C. Ke, B.Z. Tang, Journey of aggregation-induced emission research, *ACS Omega* 3 (3) (2018) 3267–3277.
- [31] J. Mei, N.L.C. Leung, R.T.K. Kwok, J.W.K. Lam, B.Z. Tang, Aggregation-induced emission: together we shine, united we soar!, *Chem. Rev.* 115 (21) (2015) 11718–11940.
- [32] M. Gao, B.Z. Tang, Fluorescent sensors based on aggregation-induced emission: recent advances and perspectives, *ACS Sens.* 2 (10) (2017) 1382–1399.
- [33] J. Shi, Y. Li, Q. Li, Z. Li, Enzyme-responsive bioprobes based on the mechanism of aggregation-induced emission, *ACS Appl. Mater. Interfaces* 10 (15) (2018) 12278–12294.
- [34] G. Jiang, G. Zeng, W. Zhu, Y. Li, X. Dong, G. Zhang, X. Fan, J. Wang, Y. Wu, B.Z. Tang, A selective and light-up fluorescent probe for β -galactosidase activity detection and imaging in living cells based on an AIE tetraphenylethylene derivative, *Chem. Commun.* 53 (32) (2017) 4505–4508.
- [35] Z. Ruan, Y. Shan, Y. Gong, C. Wang, F. Ye, Y. Qiu, Z. Liang, Z. Li, Novel AIE-active ratiometric fluorescent probes for mercury(II) based on the Hg^{2+} -promoted deprotection of thioketal, and good mechanochromic properties, *J. Mater. Chem. C* 6 (4) (2018) 773–780.
- [36] X. Ou, X. Lou, F. Xia, A highly sensitive DNA-AIEgen-based “turn-on” fluorescence chemosensor for amplification analysis of Hg^{2+} ions in real samples and living cells, *Sci. China Chem.* 60 (5) (2017) 663–669.
- [37] Y. Chen, W. Zhang, Y. Cai, R.T.K. Kwok, Y. Hu, J.W.Y. Lam, X. Gu, Z. He, Z. Zhao, X. Zheng, B. Chen, C. Gui, B.Z. Tang, AIEgens for dark through-bond energy transfer: design, synthesis, theoretical study and application in ratiometric Hg^{2+} sensing, *Chem. Sci.* 8 (3) (2017) 2047–2055.
- [38] A. Chatterjee, M. Banerjee, D.G. Khandare, R.U. Gawas, S.C. Mascarenhas, A. Ganguly, R. Gupta, H. Joshi, Aggregation-induced emission-based chemodosimeter approach for selective sensing and imaging of $Hg(II)$ and methylmercury species, *Anal. Chem.* 89 (23) (2017) 12698–12704.
- [39] X. Wen, Z. Fan, A novel “turn-on” fluorescence probe with aggregation-induced emission for the selective detection and bioimaging of Hg^{2+} in live cells, *Sens. Actuators B Chem.* 247 (2017) 655–663.
- [40] L. Liu, G. Zhang, J. Xiang, D. Zhang, D. Zhu, Fluorescence “Turn on” chemosensors for Ag^+ and Hg^{2+} based on tetraphenylethylene motif featuring adenine and thymine moieties, *Org. Lett.* 10 (20) (2008) 4581–4584.
- [41] L.N. Neupane, E.-T. Oh, H.J. Park, K.-H. Lee, Selective and sensitive detection of heavy metal ions in 100% aqueous solution and cells with a fluorescence chemosensor based on peptide using aggregation-induced emission, *Anal. Chem.* 88 (6) (2016) 3333–3340.
- [42] N. Zhao, J.W.Y. Lam, H.H.Y. Sung, H.M. Su, I.D. Williams, K.S. Wong, B.Z. Tang, Effect of the counterion on light emission: a displacement strategy to change the emission behaviour from aggregation-caused quenching to aggregation-induced emission and to construct sensitive fluorescent sensors for Hg^{2+} detection, *Chem. Eur. J.* 20 (1) (2014) 133–138.
- [43] H. Zhou, J. Mei, Y.-A. Chen, C.-L. Chen, W. Chen, Z. Zhang, J. Su, P.-T. Chou, H. Tian, Phenazine-based ratiometric Hg^{2+} probes with well-resolved dual emissions: a new sensing mechanism by vibration-induced emission (VIE), *Small* 12 (47) (2016) 6542–6546.
- [44] Y. Jiang, Y. Chen, M. Alrashdi, W. Luo, B.Z. Tang, J. Zhang, J. Qin, Y. Tang, Monitoring and quantification of the complex bioaccumulation process of mercury ion in algae by a novel aggregation-induced emission fluorogen, *RSC Adv.* 6 (102) (2016) 100318–100325.
- [45] R. Zhang, P. Li, W. Zhang, N. Li, N. Zhao, A highly sensitive fluorescent sensor with aggregation-induced emission characteristics for the detection of iodide and mercury ions in aqueous solution, *J. Mater. Chem. C* 4 (44) (2016) 10479–10485.
- [46] G. Huang, G. Zhang, D. Zhang, Turn-on of the fluorescence of tetra(4-pyridylphenyl)ethylene by the synergistic interactions of mercury(II) cation and hydrogen sulfate anion, *Chem. Commun.* 48 (60) (2012) 7504–7506.
- [47] W. Fang, G. Zhang, J. Chen, L. Kong, L. Yang, H. Bi, J. Yang, An AIE active probe for specific sensing of Hg^{2+} based on linear conjugated bis-Schiff base, *Sens. Actuators B Chem.* 229 (2016) 338–346.
- [48] K. Ma, X. Li, B. Xu, W. Tian, A sensitive and selective “turn-on” fluorescent probe for Hg^{2+} based on thymine- Hg^{2+} -thymine complex with an aggregation-induced emission feature, *Anal. Methods* 6 (7) (2014) 2338–2342.
- [49] M.T. Gabr, F.C. Pigge, A turn-on AIE active fluorescent sensor for Hg^{2+} by combination of 1,1-bis(2-pyridyl)ethylene and thiophene/bi thiophene fragments, *Mater. Chem. Front.* 1 (8) (2017) 1654–1661.
- [50] Q. Lin, X.-M. Jiang, X.-Q. Ma, J. Liu, H. Yao, Y.-M. Zhang, T.-B. Wei, Novel bispillar [5]arene-based AIEgen and its application in mercury(II) detection, *Sens. Actuators B Chem.* 272 (2018) 139–145.
- [51] M. Shyamal, S. Maity, A. Maity, R. Maity, S. Roy, A. Misra, Aggregation induced emission based “turn-off” fluorescent chemosensor for selective and swift sensing of mercury (II) ions in water, *Sens. Actuators B Chem.* 263 (2018) 347–359.
- [52] Y. Li, Y. Liu, H. Zhou, W. Chen, J. Mei, J. Su, Ratiometric Hg^{2+}/Ag^+ probes with orange red-white-blue fluorescence response constructed by integrating vibration-induced emission with an aggregation-induced emission motif, *Chem. Eur. J.* 23 (39) (2017) 9280–9287.
- [53] H.-B. Cheng, Z. Li, Y.-D. Huang, L. Liu, H.-C. Wu, Pillararene-based aggregation-induced-emission-active supramolecular system for simultaneous detection and removal of mercury(II) in water, *ACS Appl. Mater. Interfaces* 9 (13) (2017) 11889–11894.
- [54] G. Jiang, J. Wang, Y. Yang, G. Zhang, Y. Liu, H. Lin, G. Zhang, Y. Li, X. Fan, Fluorescent turn-on sensing of bacterial lipopolysaccharide in artificial urine sample with sensitivity down to nanomolar by tetraphenylethylene based aggregation induced emission molecule, *Biosens. Bioelectron.* 85 (2016) 62–67.